Title

The evolution of antimicrobial peptide resistance in *Pseudomonas aeruginosa* is severely constrained by random peptide mixtures

Authors

B. Antunes[1,2,*], C. Zanchi[1,*], P.R. Johnston[1,3], B. Maron[2], C. Witzany[4], R. Regoes[4], Z. Hayouka[2,#] and J. Rolff[1, #]

[1] Freie Universität Berlin, Evolutionary Biology, Königin-Luise-Straße 1-3, 14195 Berlin, Germany.

[2] Institute of Biochemistry, Food Science and Nutrition, The Hebrew University of Jerusalem, Rehovot, Israel.

[3] Berlin Centre for Genomics in Biodiversity Research, Berlin, Germany

[4] Institute of Integrative Biology, ETH Zurich, Zurich, Switzerland.

* Co-first authors.

[#] Corresponding authors: Zvi Hayouka (zvi.hayouka@mail.huji.ac.il) and Jens Rolff (jens.rolff@fu-berlin.de).

Abstract

The prevalence of antibiotic-resistant pathogens has become a major threat to public health, requiring swift initiatives for discovering new strategies to control bacterial infections. Hence, antibiotic stewardship and rapid diagnostics, but also the development, and prudent use, of novel effective antimicrobial agents are paramount. Ideally, these agents should be less likely to select for resistance in pathogens than currently available conventional antimicrobials. The usage of antimicrobial Peptides (AMPs), key components of the innate immune response, and combination therapies, have been proposed as strategies to diminish the emergence of resistance.

Herein, we investigated whether newly developed random antimicrobial peptide mixtures (RPMs) can significantly reduce the risk of resistance evolution *in vitro* to that of single sequence AMPs, using the ESKAPE pathogen *Pseudomonas aeruginosa* (*P. aeruginosa*) as a model Gram-negative bacterium. Infections of this pathogen are difficult to treat due the inherent resistance to many drug classes, enhanced by the capacity to form biofilms. *P. aeruginosa* was experimentally

evolved in the presence of AMPs or RPMs, subsequentially assessing the extent of resistance evolution and cross-resistance/collateral sensitivity between treatments. Furthermore, the fitness costs of resistance on bacterial growth were studied, and whole-genome sequencing used to investigate which mutations could be candidates for causing resistant phenotypes. Lastly, changes in the pharmacodynamics of the evolved bacterial strains were examined.

Our findings suggest that using RPMs bears a much lower risk of resistance evolution compared to AMPs and mostly prevents cross-resistance development to other treatments, while maintaining (or even improving) drug sensitivity. This strengthens the case for using random cocktails of AMPs in favour of single AMPs, against which resistance evolved *in vitro*, further providing an alternative to classic antibiotics worth pursuing.

Introduction

The prevalence of antibiotic-resistant pathogens has become a major threat to public health, with an estimated 4.95 million deaths associated with drug-resistant bacteria in 2019 (1). Although resistance is a natural development, misuse and overuse of antibiotics has accelerated evolutionary selection and resistance, decreasing the efficiency of available antibiotics (2, 3). Hence, there is a strong incentive to discover new strategies to control bacterial infections, such as antibiotic stewardship and rapid diagnostics, but also the development, and prudent use, of novel effective antimicrobial agents (4, 5). An important and desirable feature of such agents would be a much lower risk to select for drug resistance in pathogens than currently available conventional antimicrobials. This would make the use of such drugs much more sustainable.

Antimicrobial Peptides (AMPs) form an important component of the innate immune response in multicellular organisms and have been frequently proposed as new antimicrobial drug candidates (6). These peptides usually have spatially explicit hydrophobic and cationic residues, which promote their ability to disrupt bacterial membranes (7, 8). Fundamentally, while hydrophobic residues interact with the hydrophobic interior of the lipid bilayer, their high net cationic charge selects prokaryotic membranes over eukaryotic cells (9, 10). AMPs range across the tree of life, showing a surprising diversity and variety in size and form (11). Moreover, while resistance has been shown to evolve against these antimicrobial agents, it evolves at a much slower rate than conventional antibiotics (12-14). Interestingly, for colistin, an AMP of bacterial origin that has been

61 used for more than sixty years (15), it took around fifty years between the introduction and the
62 spread of resistance (16).
63 In the current antibiotic crisis, bacterial pathogens are increasingly resistant to the available
64 monotherapeutical antibiotic drugs, often evolved through redundant mechanisms and to multiple
65 antibiotics in the same organism (17). This situation has been exacerbated by misuse and lack of
66 innovation in the discovery of new, and effective, antibiotic agents (18). Hence, combination
67 therapies have been explored and shown, by multitarget engagement, to diminish the emergence
68 of spontaneous resistance (19, 20). Among novel strategies under scrutiny is the usage of newly
69 developed random antimicrobial peptide mixtures (RPMs) (21, 22).
70 The broad molecular diversity of AMPs suggests that their prokaryotic-selective activity does not
71 depend on specific features of amino acid sequence or peptide conformation (8). Hence, research
72 groups have developed novel approaches to synthesize RPMs, using a solution containing
73 defined concentrations of hydrophobic and cationic amino acids (21, 23). This results in 2^n peptide
74 sequences (where n is the number of coupling steps and the chain length of the peptides). These
75 random peptide libraries, composed of hydrophobic and cationic amino acids, have shown strong
76 antimicrobial activity against multiple gram-negative and positive bacteria, including multi-drug
77 resistant (MDR), methicillin-resistant *Staphylococcus aureus* (MRSA), vancomycin-resistant
78 *Enterococci* (VRE), *Listeria monocytogenes* and several plant pathogenic bacteria (24-27).
79 Moreover, some attention has been given to a subfamily of AMPs with strong antimicrobial activity
80 – lipopeptides. Lipopeptides are produced non-ribosomally in bacteria and fungi, consisting of a
81 short linear or cyclic peptide sequence to which a fatty acid moiety is covalently attached at the
82 N-terminus (28). Synthetic ultrashort lipopeptides have shown broad antimicrobial activity towards
83 human pathogenic yeast, fungi and bacteria, as well as plant pathogenic fungi and bacteria (29,
84 30). RPMs of synthetic lipopeptides have also been studied by Topman-Rakover et al., displaying
85 broad antimicrobial activity against gram-negative and gram-positive bacteria, without causing
86 cytotoxicity to mammalian cells or plants (25, 26).
87 Here, we studied whether a treatment strategy based on the usage of RPMs and lipo-RPMs, can
88 significantly reduce the risk of resistance evolution *in vitro*, compared to AMPs. We used the
89 ESKAPE pathogen *Pseudomonas aeruginosa* (*P. aeruginosa*) as a model gram-negative
90 bacterium (31). This opportunistic pathogen is involved in chronic respiratory infections,

particularly those associated with cystic fibrosis, as well as hospital-acquired infections (32). *P. aeruginosa* infections are difficult to treat due the inherent resistance to many drug classes, enhanced by the capacity to form sessile microcolonies that stick to a surface and each other, eventually forming biofilms (33, 34). Resistance associated *P. aeruginosa* deaths were estimated around 300 thousand in 2019 (1).

We allowed *P. aeruginosa* to experimentally evolve in the presence of AMPs or RPMs. The selection covered 4 weeks, which is consistent with treatment regimens of *P. aeruginosa* infections (35). At the end of the experimental evolution course, we measured the extent of resistance evolution and whether the evolved strains showed cross-resistance/collateral sensitivity to the AMPs and RPMs. We also assessed the fitness costs of resistance on bacterial growth, and used whole-genome sequencing to investigate which mutations could be candidates for causing resistant phenotypes. Finally, we investigated changes in the pharmacodynamics of the evolved bacterial strains (12, 36, 37).

The usage of random peptide libraries (i.e. RPMs) instead of homogeneous peptides (i.e. one sequence, one chain length and one stereochemistry) offers some practical advantages, as the chemical synthesis of sequence-specific oligomers is more difficult and expensive than copolymerization (21). Hence, this study aims not only to provide in-depth insight on RPMs as novel alternatives to classical antibiotics, but also to how they fare in comparison to single sequence AMPs. Our findings suggest that using RPMs results in a much lower probability of resistance evolution and mostly prevents cross-resistance development to other treatments, while maintaining (or even increasing) drug sensitivity.

Results

1. <u>RPMs slow down resistance evolution.</u>

The evolution of resistance in *P. aeruginosa 14* (PA14) was investigated against nine antimicrobials: 6 single sequence AMPs and 3 RPMs, with diverse modes of action, all active against PA14 (by standard MIC assays; Table S1). The level of resistance was determined based on the change of the MIC of the evolved strains in comparison to the previously determined MIC of the ancestor strain ("MIC fold-change"; Table S1). The selection regime was found to influence MIC fold-changes across the different evolved strains ($X^2_{17.88}$=565.4; $p<0.0001$; Fig. 1 and S5).

121 We found that all AMPs select for resistance when compared to their respective control (i.e. MIC
122 fold-change is significantly different from the MIC fold-change of the control, when exposed to the
123 same AMP). Among the RPMs, only p-FdK5 20/80 showed a significant difference compared to
124 the control. The magnitude of the difference between evolved and control is much lower for the 3
125 RPMs compared to all the single sequence AMPs.

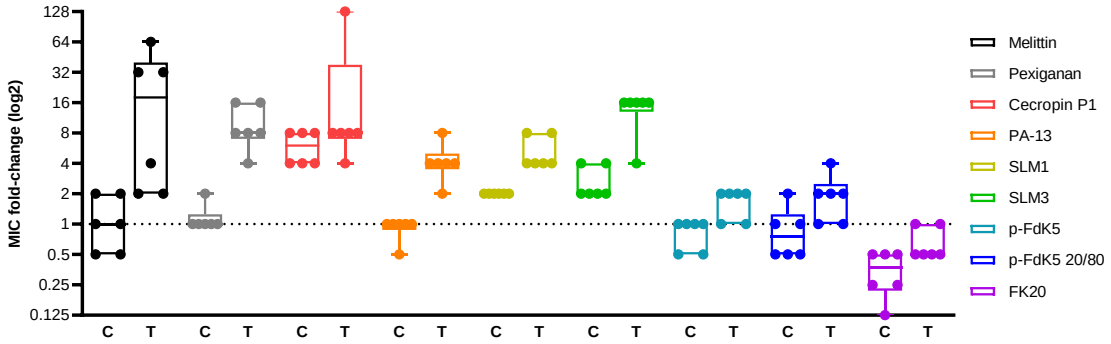

126 *Figure 1 – Resistance evolves slower in RPMs, when compared with single sequence AMPs. Resistance*
127 *determined by MIC assay of each evolved strain towards the corresponding peptide ("T" represents*
treated groups and "C" the control exposed to the respective treatment). Results shown as log2 fold-
128 *change of the ancestor MICs. The boxes span the range between the 25th and 75th percentile, while the*
horizontal line inside represents the median value. The vertical bars extend to the minimum and
129 *maximum score, excluding outliers (n=6; $X^2_{17,88}$ = 565,4; p<0.0001). The results represent two*
independent experiments.

130 Additionally, under this experimental setting, the resistance to Cecropin P1 seems to evolve
131 readily, as the control strain showed a significantly higher MIC fold-change when exposed to
132 Cecropin P1 than in any other AMPs/RPMs-exposed control. The opposite effect can be seen in
133 the FK20 treatment, in which the control strain shows the lowest MIC fold-change.
134 Overall, FK20 out-performed all the other peptides in hindering resistance evolution, including
135 both 5-mer lipo-RPMs p-FdK5 and p-FdK5 20/80. Among single sequence AMPs, PA-13 and
136 SLM1 performed best, leading to a lower MIC fold-change compared to the other AMPs. *Post hoc*
137 analysis shows that RPMs reduce resistance evolution better than single sequence AMPs (Fig.
138 S5), particularly evident for FK20-evolved strains.

139 2. <u>Most evolved strains display collateral sensitivity to FK20.</u>

140 In the case of cross-resistance, evolution of resistance to one drug can increase bacterial fitness
141 to other drugs, while the opposite is known as collateral sensitivity (38, 39). To investigate this in
142 our experimentally evolved strains, they were exposed to the other antimicrobials of our panel
143 (Fig. 2). Across the board, strains evolved against Melittin, Pexiganan, Cecropin P1 and PA13
144 retained sensitivity to FK20, as did strains evolved in the presence of FK20. Furthermore,
145 Cecropin P1-evolved strains, despite being resistant to Cecropin P1, did not show cross-

146 resistance towards Melittin, Pexiganan and PA-13. On the other hand, strains evolved in the
147 presence of Melittin and Pexiganan, PA13 and FK 20 were cross-resistant to Cecropin P1, the
148 most resistant strains being the ones evolved in the presence of Melittin and Pexiganan.

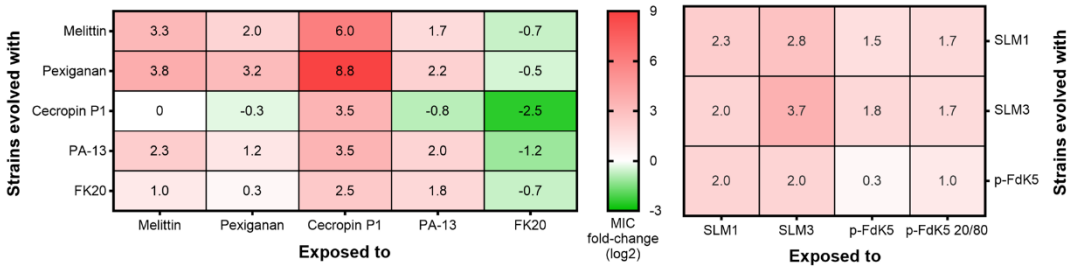

149

150 *Figure 2 – Cross-resistance evolved frequently against Cecropin P1, but collateral sensitivity steadily evolved towards FK20. A standard MIC assay was performed to evaluate the cross-resistance and*
151 *collateral sensitivity. In each experiment, the evolved strains were exposed to different AMPs/RPMs, using the selected AMP/RPM as control. The MIC values are represented as the mean fold-change (log2)*
152 *of the ancestor's MIC. The results represent two independent experiments (n=6). Red colour represents cross-resistance and green indicates collateral sensitivity.*

153 Cross-resistance/collateral sensitivity of bacterial strains evolved in the presence of lipopeptides
154 against other lipopeptides of our panel (SLM1, SLM3 and lipo-RPMs p-FdK5 and p-FdK5 20/20)
155 was also evaluated. We detected no observable collateral sensitivity towards the remaining
156 palmitic acid-modified peptides (Fig. 2). Nonetheless, despite great amino acid sequence
157 similarity between peptides (Table S1), only moderate levels of cross-resistance were observed
158 for lipo-AMPs/-RPMs. Nonetheless, the level of cross-resistance between palmitic acid modified
159 peptides is of far lesser magnitude than the level of cross-resistance towards Cecropin P1
160 exhibited by strains selected for other peptides.

161 3. <u>Lower resistance evolution leads to extended lag time.</u>

162 The fitness cost associated with the evolution of PA14 in presence, or absence, of AMP/RPMs
163 was investigated and the parameters, lag time and maximum growth rate (Vmax), were
164 normalised to those of the ancestor strain (i.e. fold-change; Fig. S1). There was a significant effect
165 of the selection regime on the lag time fold-change (Fig. S1-A; $X^2_{9,40} = 44,31$; $p<0.0001$), namely,
166 Pexiganan-, PA-13-, SLM3- and FK20-evolved strains display significantly increased lag times,
167 compared to control strains (Fig. S1-A and S6). There was, however, no effect of the experimental
168 evolution regime on the maximum growth rate (Vmax) of the strains (Fig. S1-B; $X^2_{9,40} = 11,9$;
169 $p=0.22$).

170

4. Mutations evolved in all treatments.

To better understand the mechanisms responsible for resistance evolution (or absence thereof), the genomic DNA of evolved strains was sequenced and compared to the assembled genome of the ancestor strain of PA14. A heat-map summary of the emerged mutations in evolved strains (including control) can be found in Fig. S2. Sequencing revealed that the majority of occurring SNPs were present in five genes (84%): *lasR*, *phoQ*, *tpbB*, *oprL* and *wbpA* (Fig. 3; strains without mutations were also plotted for comparison). In this section, cross-resistance/collateral sensitivity data was used to explore whether the SNPs in these 5 genes were associated with resistance to the panel of tested antimicrobials. Specifically, we tested whether presence/absence of a SNP, in each of the 5 genes, explained MIC fold-changes towards individual antimicrobial treatments, among the bacterial strains of all selection regimes. Interestingly, among these 5 genes, *tpbB* and *oprL* presented SNPs in only 1 of the 2 replicates of the experiment. Additionally, the software tool Provean was used to predict whether an amino acid substitution, or indel, affected the biological function of the target protein (40).

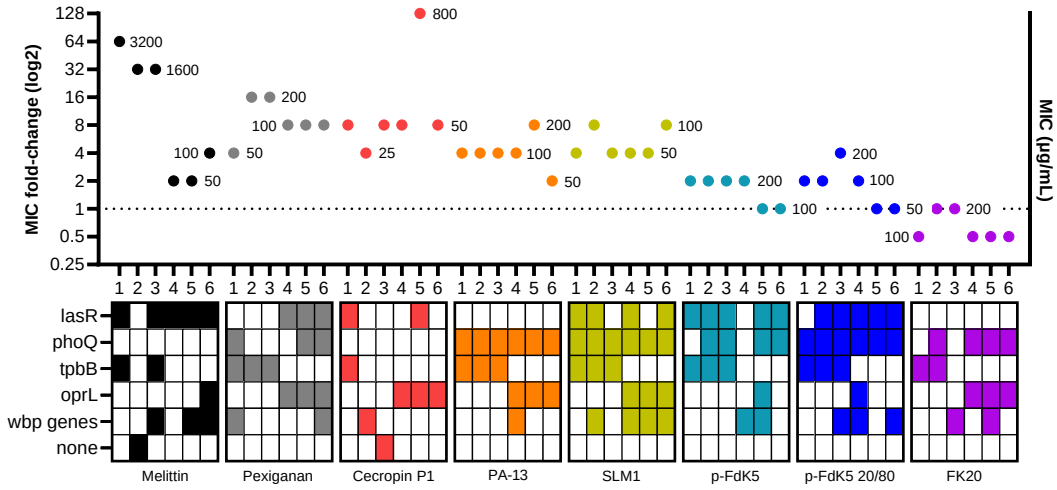

Figure 3 – Representation of the resistance evolution (MIC fold-changes) in relation to the presence/absence of mutations in the 5 most frequently mutated genes. Results shown as log2 fold-change of the ancestor MICs; Each dot represents the mean of triplicates (values beside the dots represent the MIC value). The x-axis displays individual strains per treatment and the respective mutations (or absence of) are portrayed underneath. The results represent two independent experiments. Evolved mutations against FK20 did not result in resistant strains.

TpbB is a diguanylate cyclase which is directly involved in the formation small colony variants (SCVs) in P. aeruginosa (41). A single type of SNPs was found in the *tpbB* gene, resulting in an amino acid substitution (valine to alanine in position 40), deemed not to affect protein function by

192 Provean. *TpbB* gene mutations only evolved in the strains of the first replicate of the experiment,
193 but across most of them (22 out of 27 sequenced strains), and across all treatments, including
194 the control. Within the 1st replicate of the experiment, the presence of this SNP in *tpbB* did not
195 explain MIC fold-change towards any of the tested antimicrobials (Fig. S8 and Table S3).
196 On the other hand, SNPs in the *oprL* gene, a membrane lipoprotein which plays an important role
197 in the interaction of *P. aeruginosa* with the environment (42), evolved only in strains of the second
198 replicate of the experiment. SNPs in *tpbB*, in the *orpL* gene they were found in most strains (20
199 out of 27), and across all treatments including the control. Unlike *tpbB*, however, SNPs found in
200 *oprL* (leucine replaced by a phenylalanine in position 43) are predicted to impair protein function.
201 Thus, the presence of this SNP increased MIC fold-change towards Melittin, Pexiganan and
202 Cecropin P1 (Fig. S9 and Table S3).
203 LasR is a transcriptional regulator that controls the expression of virulence factors and biofilm
204 formation in *P. aeruginosa* (43). In our experiments, we found a high number of different SNPs in
205 the *lasR* gene, for most selection regimes, accounting for 27 different SNPs across 29 strains.
206 SNPs in *lasR* were also present in 3 out of the 6 control strains. Among these 27 different SNPs,
207 only 6 were deemed not to affect protein function by Provean, whereas the rest were deleterious.
208 Despite this feature, the presence, or absence, of SNPs in the *lasR* gene is not associated with
209 fold-changes in MIC towards any of the tested antimicrobials (Fig. S10 and Table S3).
210 We also found SNPs in several members of the *wbp* pathway leading to the synthesis of the B-
211 band O-antigen of the Lipopolysaccharide (LPS) in *P. aeruginosa* (44). The most commonly found
212 SNP was a frameshift variant of *wbpA,* while the second most commonly found was a missense
213 mutation in *wbpA*, leading to the replacement of a valine in position 32 by a glycine. The 3 SNPs
214 found in *wbpL* also caused frameshifts, as did the 4 SNPs present in the *wbpI* gene. According to
215 Provean, all these SNPs were deleterious, thus inactivating the products of the respective genes.
216 It has been shown that any missing member of this pathway led to a loss of the B-band O-Antigen
217 of LPS in *P. aeruginosa* (45). Since, *wbp* SNPs found herein were deemed deleterious, we
218 consider these together as inactivating the *wbp* pathway (named "*wbp* genes" in the figures; Fig.
219 S11). Nonetheless, we did not find these deleterious SNPs to affect MIC fold-change towards any
220 of the tested antimicrobials (Fig. S11 and Table S3). Additionally, given that such SNPs were

221 present in all treatments, including the control, once again indicates that they were unlikely to
222 have been selected by our antimicrobials.
223 Among the 5 majorly found gene mutations, only *phoQ* did not show any SNPs in the control
224 group. The *phoQ* gene codes for a Mg^{2+} sensor which is part of a two-component system that
225 controls several pathogenic properties in Gram-negative bacteria (46). In our experiments, the
226 most represented SNP in *phoQ* (in 28 strains out of 29) leads to a replacement of a valine in
227 position 260 by a glycine, which was previously associated to colistin resistance in *P. aeruginosa*
228 isolates (47). All SNPs were deemed deleterious by Provean.
229 The *phoQ* gene mutation was, in fact, the most frequently observed mutation (present in 29
230 different strains), although its distribution was not consistent throughout all the evolved strains.
231 While SNPs were present in all the strains evolved in the presence of PA13, SLM1 and p-FdK5
232 20/80, in 4 out of 6 of the p-FdK5 and FK20-selected strains and in 3 out of 6 of Pexiganan-
233 selected strains, they were absent from Melittin and Cecropin P1-selected strains, as well as the
234 control strains. Moreover, the presence of this SNP in *phoQ* is associated to a higher MIC fold-
235 change towards PA13, SLM1, SLM3, p-FdK5 and p-FdK5 20/80 (Fig. S12 and Table S3).
236 There were only 3 strains in which no SNPs were detected compared to the ancestor PA14: 1 in
237 the Melittin, 1 in the Cecropin P1 and 1 in the control selection regimes (Fig. 3 and S4). However,
238 both the Melittin- and Cecropin P1-evolved strains showed a higher resistance towards Melittin
239 and Cecropin P1 respectively. Moreover, it would have perhaps been expected to find more than
240 just one mutation-less strain in the control group, as it was evolved absent of AMP/RPMs.
241 Nonetheless, naturally occurring mutations result of continuous culturing are expected (48, 49),
242 and, in fact, wild-type PA14 was shown to have a 6.12×10^{-4} spontaneous mutation rate per
243 genome (50).

244 5. <u>The Hill coefficient evolves with the MIC.</u>

245 The steepness of the pharmacodynamic curves (i.e. the Hill coefficient, kappa; κ) generated from
246 time-kill curves provide information about the width of the mutant selection window (i.e the
247 concentration range where resistant mutants are selected for; MSW), as a higher kappa results
248 in a narrower MSW (Fig. 4A). Therefore, we analysed kappa evolution for the most resistant
249 strains, in each selection regime, by correlating it with their respective MIC fold-change (Fig. 4B).
250 The kappa value of the most resistant evolved strains was normalised to that of the ancestor, for

each AMP/RPM. Six out of eight AMP/RPMs can be found in the lower-right quadrant of MIC fold-change and kappa fold-change correlation (Fig. 4B), therefore not only evolving resistance to PA14, but also generating a lower kappa than that of the ancestor strain. Indeed, a Spearman's correlation shows an inverse relationship between MIC and kappa fold-change (ρ= -0.8743; p-value=0.0045), where a lower kappa correlates to a higher MIC, except for p-FdK5-evolved strains.

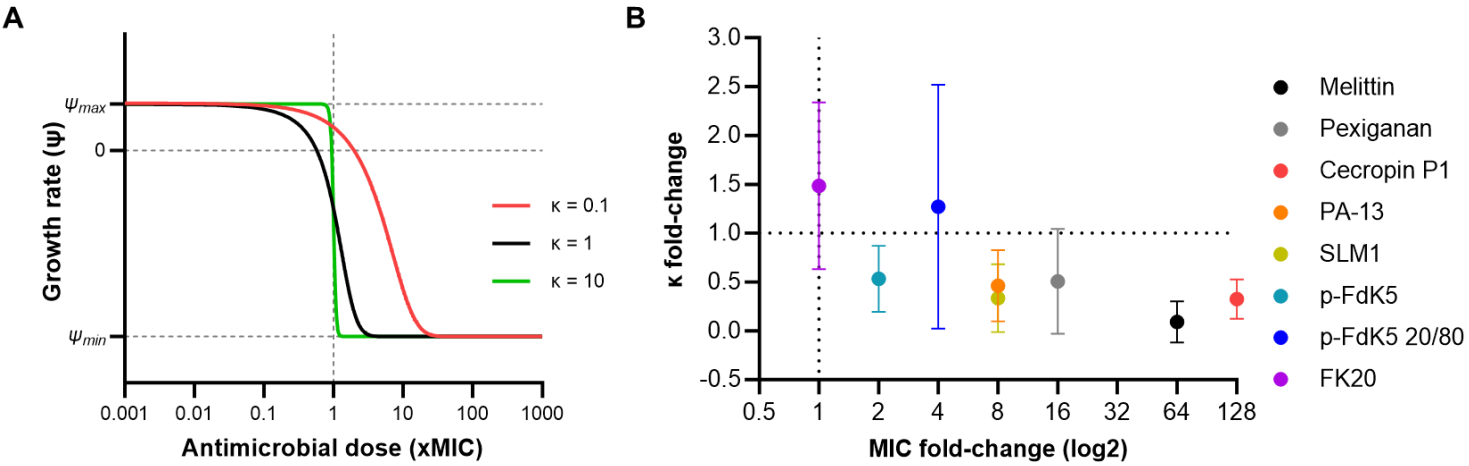

Figure 4 – (A) Schematic illustration of the four parameters predicted by the Hill function: zMIC, ψ_{max}, ψ_{min}, and κ. The zMIC is estimated by the lowest concentration that inhibits the growth of the whole treated bacterium population. While ψ_{max} represents the maximal growth rate of bacteria (i.e. in absence of antimicrobials), ψ_{min} represents the minimal bacterial growth rate, or maximal killing rate of the antimicrobial treatment. The Hill coefficient, κ, predicts the shape and slope of the pharmacodynamic curve; the higher κ is, the steeper the pharmacodynamic curve. Pharmacodynamic curves are represented in different colours (i.e. red, black and green) to portray the change in slope and MIC values.

(B) The MIC and Hill coefficient (κ) of selected strains seem to evolve in correlational fashion. Graphic representing the correlation between evolution of resistance evolution and kappa (ρ=-0,8743; p-value=0,0045). Resistance determined by MIC assay of each strain toward the corresponding peptide, shown as log2 fold-change of the ancestor MICs. Evolution of kappa determined by Hill function-based Rstan model, shown as fold-change of the ancestor's kappa. Each dot represents the mean of triplicates.

Using p-FdK5 20/80, despite evolving resistance, generated a slightly higher κ compared to that of the ancestor strain, therefore maintaining the sensitivity towards the evolved strains. As previously seen (Fig. 1), only under FK20 selection could resistance evolution not be observed, during the 4 weeks under selection, yet it resulted in a higher kappa compared to the that of the ancestor (Fig. 4B).

Discussion

The present work was primarily motivated by a growing necessity and interest in exploring novel alternatives to conventional antibiotics. By using a combined approach of experimental evolution,

274 pharmacodynamic modelling and genome re-sequencing, we show how novel random peptide
275 libraries compare to single AMPs in respect to antimicrobial resistance evolution. AMPs have
276 been gaining attention for their potential as antimicrobial agents, partly because of the low
277 probability of resistance evolution (7, 8, 10, 51). In fact, the WHO reported that 15.2% of
278 antibacterials in the preclinical pipeline are AMPs (52), a notable increase from 10.7% reported
279 in the previous review (53). Our hypothesis was that RPMs, as a cocktail of multiple AMPs, would
280 represent an increased set of challenges for bacteria to overcome compared to single AMPs,
281 potentially delaying resistance evolution.
282 Having selected a broad array of AMPs and RPMs, shown to be active against PA14 *via* MIC
283 determination (Table S1), we saw that resistance evolved against the great majority (2 to 128-fold
284 MIC increase; Fig. 1). These observations are consistent with previous evidence showing that
285 despite lower probability of resistance evolution against AMPs compared to conventional
286 antibiotics, *in vitro* resistance evolution towards AMPs can evolve (13, 54, 55). Conversely, it was
287 observed that random peptide libraries (RPMs), based on cationic and hydrophobic moieties, can
288 significantly delay, or avoid, resistance evolution when compared to single sequence AMPs (Fig.
289 1 and S5). While palmitic acid-modified RPMs, p-FdK5 and p-FdK5 20/80, were able to greatly
290 reduce the magnitude of resistance evolution, FK20 was the only one effectively escaping it within
291 the context of our experimental setting (Fig. 1). The selection setting herein used covered 4
292 weeks, which is consistent with treatment regimens of *P. aeruginosa* infections (35).
293 Random peptide libraries encase a cocktail of AMPs. Whereas FK20, a 20-mer, can produce over
294 1 million AMP combinations (2^{20}), p-FdK5 and p-FdK5 20/80, although modified with palmitic acid
295 for increased hydrophobicity, being 5-mers, provide less AMP combination possibilities (32 and
296 less, respectively) (21, 22, 26). Hence, the availability of a cocktail of multiple AMPs seems to
297 favour the usage of RPMs, as it creates an increased set of challenges for bacteria to overcome,
298 which can potentially delay resistance evolution. However, drug combinations (including AMPs)
299 should be carefully planned, to avoid the risk of leading to formulations that are inferior to using
300 single agents. Pena-Miller et al. make an interesting case when trying to achieve optimal
301 synergistic effects in drug combinations (56): synergy can exert strong selection for resistance,
302 leading to consistent antagonistic emergence. Thus, unless super-inhibitory doses are applied

303 until the pathogen is successfully cleared, synergistic antibiotics could have the opposite effect
304 and lead to increased pathogen load.
305 Analysis of the cross-resistance/collateral sensitivity results (Fig. 2) revealed some interesting
306 patterns. Cecropin P1-evolved strains show collateral sensitivity to Pexiganan, PA-13 and FK20.
307 Conversely, Pexiganan, PA-13 and FK20-evolved strains show cross-resistance to Cecropin P1.
308 Remarkably, all evolved strains show collateral sensitivity to FK20, which could potentially lead to
309 a positive impact on single AMPs if combined with FK20. In fact, several studies have proposed
310 collateral sensitivity as a promising strategy to slow down the resistance evolution process and
311 even reverse the pre-existing resistance (39, 57-59). Imamovic and collaborators demonstrated
312 that resistance evolution to *P. aeruginosa* for antibiotics used in cystic fibrosis patients caused
313 collateral sensitivity to other antibiotics (39). The study showed that the optimized drug treatment,
314 based on the collateral sensitivity interactions, effectively eradicated the resistant subpopulation
315 from the patient's lungs.
316 In line with previous studies, growth parameters lag time and maximum growth rate (Vmax) were
317 used to estimate cost of resistance evolution (14, 60). Our investigation revealed that strains
318 evolved in the presence of Pexiganan, PA-13, SLM3 and FK20 displayed a fitness cost, resulting
319 in significantly increased lag times compared to control (Fig. S1-A). This result is surprising in the
320 case of FK20-evolved strains, which did not evolve resistance. There were no differences
321 between the lag time of the ancestor and the procedural controls after selection (Fig. S1-A), thus
322 adaptation to the experimental conditions did not affect this aspect of the bacterial fitness. Ward
323 and associates (61) have shown that, clinically isolated MDR strains of *P. aeruginosa* frequently
324 have similar fitness in the absence of antibiotics. Therefore, under certain circumstances, using
325 AMP formulations against which resistance evolution is more costly, might be more effective in
326 preventing resistance evolution, though the relationship between cost and resistance is not
327 always strong (62).
328 No selection regime significantly affected Vmax compared to control, however, the Vmax of the
329 control groups was higher than that of the ancestor (Fig. S1-B). Faster growth rates than that of
330 the ancestor strain have been shown to result from adaptation to a serial passaging environment
331 (63, 64), due to an enhanced ability to acquire, or more efficiently utilize available nutrients during
332 post-exponential growth. On the other hand, no significant differences in Vmax were found

333 between experimentally evolved strains, in either treated or control regimes (Fig. S1-B). A study
334 that induced bacterial resistance to Tachyplesin I (including in *P. aeruginosa*) similarly revealed
335 that resistance acquisition did not markedly affect Vmax, in comparison to the control, but did
336 extend the lag phase (65). The authors argue that AMP resistance might compromise bacterial
337 fitness in different ways, not necessarily affecting the maximum growth rate.
338 We further studied which mutations evolved in our experimental selection treatments. By finding
339 new mutations that emerge in parallel, independently propagated lines of bacterial strains
340 exposed to antibiotics in controlled environments, are likely the cause of new heritable resistant
341 genotypes (66). Among the five genes comprising most of the SNPs in our dataset, *phoQ* was the
342 only one for which SNPs did not evolve in the control lines, suggesting that it evolved as a
343 response to a selection pressure exerted by some of the antimicrobials of our panel. This SNP
344 results in the substitution of a valine by a glycine in position 260 (Histidine kinase A domain),
345 which was deemed to abolish protein function by Provean. This same SNP has also been
346 previously reported to lead to loss-of-function of the PhoQ protein, leading to an increased
347 resistance to colistin in *P. aeruginosa* by Lee and Ko (47).
348 In *P. aeruginosa*, adaptive resistance to cationic AMPs is known to occur in response to limiting
349 extracellular concentrations of Mg^{2+} and Ca^{2+} cations (67, 68). This adaptation is controlled by
350 two-component regulators PhoP-PhoQ and PmrA-PmrB which upregulate the expression of the
351 *arnBCADTEF* lipopolysaccharide (LPS) modification operon (68). The products of these *arn*
352 genes lead to reducing the net negative charge of LPS, limiting the interaction and self-promoted
353 uptake of polycationic antibiotics (e.g. AMPs and aminoglycosides). *PhoQ* expression allows for
354 the integration of environmental cues when bacterial density is high and nutritional resources are
355 rarefied (69). Inactivation of *phoQ* ultimately lead to constitutive LPS modifications which have
356 been shown to confer *P. aeruginosa* colistin resistance (70).
357 *PhoQ* SNPs were present in all evolved treatments, except Melittin and Cecropin P1-selected
358 strains. Moreover, the presence of this SNP in *phoQ* is associated to a higher MIC fold-change
359 towards PA13, SLM1, SLM3, p-FdK5 and p-FdK5 20/80 (Fig. S12). Interestingly, given that *phoQ*
360 SNPs were not found in Melittin and Cecropin P1-evolved strains, the only antimicrobial-selected
361 group with the *phoQ* mutation, which was not associated with higher MIC fold-change is FK20.

362 Therefore, FK20 is the only selection regime in which the presence of this SNP in the *phoQ* gene
363 was not associated to a higher MIC fold-change.
364 SNPs found in the 4 other genes (*lasR*, *wbp*- genes, *tpbB* abd *oprL*) were also detected in the
365 strains of the control selection regime, which means that antimicrobials are unlikely to have
366 selected for their emergence in our bacterial strains.
367 We found a high number of different SNPs in the *lasR* gene (mostly predicted to be deleterious)
368 in the bacterial strains, although the presence of these SNPs did not affect MIC fold-change
369 towards any of the tested antimicrobials in our experimental setting (Fig. S10). LasR has been
370 shown to play an important role in resistance evolution as part of P. aeruginosa quorum sensing
371 (QS) (71). The *P. aeruginosa* QS circuitry is comprised of at least two complete systems, LasR–
372 LasI and RhlR–RhlI (72). Here, the transcriptional regulator LasR controls the expression of
373 virulence factors, such as elastase LasB17, exotoxin A, pyocyanin and EPS, important players
374 for resistance evolution in *P. aeruginosa* (73). Notably, polymorphic populations of *P. aeruginosa*
375 comprising various mutants for *lasR* are selected first in patients with chronic obstructive
376 pulmonary disease (74). Yet, despite this crucial involvement in resistance, accumulation of SNPs
377 in the *lasR* gene have been shown to be widespread in *P. aeruginosa* isolated from various
378 environments, and in the absence of a distinct selection pressure (75). These previous findings
379 are confirmed in our present study. Interestingly, however, SNPs in *lasR* were absent from strains
380 evolved in the presence of PA13 and FK20, which might indicate a constraint on quorum sensing
381 function imposed by these 2 antimicrobials during evolution.
382 The biosynthesis of the B-band O-antigen of LPS is product of genes in the *wbp* pathway, among
383 which are *wbpA*, *wbpI* and *wbpL* (76). The loss of one gene product in this pathway leads to loss-
384 of-function of the B-band O-antigen at the cell surface (45). We found all SNPs in *wbpA*, *wbpI* and
385 *wbpL* (named "*wbp* genes") to be deleterious, thus it is likely that in our experiments the bacterial
386 strains presenting such a SNP do not possess the B-band O-antigen of LPS. This molecule has
387 been shown to play a critical role in host colonization, providing resistance to both serum
388 sensitivity and phagocytosis (77-79), whereas mutants of *P. aeruginosa* deficient in O-antigen
389 synthesis, are sensitive to the killing effects of human serum-mediated lysis (80).
390 With the emergence of mucoid *P. aeruginosa* within the lungs of CF patients, there are cell surface
391 changes with respect to LPS phenotype, characterized by minor expression or complete lack of

392 B-band O-antigen, while the level of A-band is maintained (78). Once *P. aeruginosa* has colonized
393 the lungs, these LPS modifications are probably beneficial for evasion of host defences (A band
394 is less immunogenic) and for alteration of susceptibility to antibiotics, since loss of B-band O-
395 antigen confers resistance to aminoglycosides (81). Thus, given that we found *wbp* pathway
396 SNPs in every evolved treatment, including the control, and that they do not explain MIC fold-
397 change, one could propose that these gene mutations resulted from an adaptation to a biofilm
398 environment, rather than from selection by the panel of antimicrobials tested.
399 We found a SNP in the tpbB gene (also called yfiN), coding for a diguanylate cyclase which
400 regulates the output of messenger cyclic-di-GMP (c-di-GMP) (82), in only 1 of the 2 experimental
401 blocks. (Fig. S8). Several *Pseudomonas* strains (including PA14) undergo phenotypic
402 diversification while adapting to the biofilm environment, forming small colony variants (SCVs)
403 (82). Strong evidence has linked SCVs formation to elevated levels of messenger cyclic-di-GMP
404 (c-di-GMP), associated with sessile phenotypes, expressing biofilm formation and attachment
405 factors (83). Resistant *P. aeruginosa* SCVs phenotype have been shown to inactivate *yfiR* and
406 *tpbA*, negative regulators of *tpbB*, leading to increased biofilm production (84). In our
407 experimentally evolved strains, the SNP in *tpbB* was found to be neutral, which might explain why
408 no effect of this SNP on the MIC-fold change was detected towards any of the tested
409 antimicrobials (Fig. S8).
410 SNPs in the *oprL* gene were also present in all selection regimes, but only in the second replicate
411 of the experiment. They consist of a leucine substitution by a phenylalanine in position 43, leading
412 to protein inactivation. OprL is the second most abundant outer membrane protein in *P.*
413 *aeruginosa*, equivalent of the *E. coli* peptidoglycan-associated lipoprotein (85). Together with
414 small lipoprotein OprI, OprL interacts with peptidoglycans, maintaining cell integrity (85), offering
415 protection from oxidative stress (86), and contributing to antibiotic resistance mechanisms in *P.*
416 *aeruginosa* by adjusting membrane permeability and multidrug efflux pumps, which secrete the
417 drugs directly out of the cell (87). In the experimentally evolved strains of this study, the presence
418 of this deleterious SNP in the *oprL* gene correlated with a higher MIC fold-change towards Melittin-
419 , Pexiganan- and Cecropin P1- evolved strains (Fig. S9).
420 Altogether, our data points to the efficiency of FK20 to slow down, or prevent, the magnitude of
421 resistance evolution of *P. aeruginosa*. A rationale to consider is that FK20 is a random peptide

422 library of over 1 million sequences, making it very difficult to evolve resistance and hence
423 resistance evolution against FK20 was not discovered within the four-week selection time span
424 in our experiment. In fact, the goal of using multiple antimicrobials would be to achieve a combined
425 effect, leading to killing efficacy and/or resistance avoidance, superior to the sum of their individual
426 counterparts (i.e. synergistic interaction) (37). Synergy between AMPs is common, leading to
427 increased killing efficacy, while constraining resistance evolution, which could explain their
428 combinational occurrence in nature (6, 88, 89). The molecular mechanisms of interactions of
429 AMPs are still largely unknown (6), although it has been suggested that synergism resulting of
430 combined AMPs can form a "supermolecule" and more stable pores (90). Furthermore, pore-
431 forming peptides can also assist other coapplied transmembrane AMPs to quickly invade bacterial
432 cells and substantially interrupt the metabolism (91).
433 Insight on why antimicrobial resistance against AMPs evolves with low probabilities, or in the case
434 of FK20 with extremely low probabilities, relies on the molecular mechanisms of killing, but also
435 on the investigation of pharmacodynamics *in vitro*, such as the one portrayed herein and by others
436 (6, 92) and *in vivo* (93). Our study revealed that AMP resistance evolution in *P. aeruginosa*
437 resulted in increased MICs, except for FK20, but also that the Hill coefficient, kappa, evolves as
438 well (36). Kappa (κ) describes how sensitive the bacterial populations net growth rate is to
439 changes in antimicrobial concentration. High κ values represent steeper pharmacodynamic
440 curves (i.e. for concentrations close to the MIC, a small increase in concentration leads to a big
441 decrease in net growth). Therefore, for high κ values a given antibiotic substance (e.g. random
442 peptide libraries or AMP combinations) has a narrower range of concentrations exerting selection
443 on resistant bacteria over susceptible ones (6, 37). This leads to the idea that kappa might relate
444 to the probability of resistance evolution against AMPs (12).
445 A negative correlation between MIC fold-change and kappa fold-change revealed that, generally,
446 lower resistance evolution led to steeper pharmacodynamic curves (i.e. kappa; Fig. 4B). Similarly,
447 El Shazely et al. have previously shown a proof-of-concept study illustrating that kappa evolves
448 in *S. aureus* (92). How kappa and the actual AMP-membrane interactions are related in our
449 examples, and in fact in most, requires further study. Work by Srinivasan et al. has studied and
450 summarized possible mechanisms including cooperativity, oligomerization and aggregation of
451 AMP molecules (94).

452 Yu and colleagues have shown that MIC and kappa significantly varied between single AMPs and
453 AMP combinations (6). As numbers of AMPs increased in combination, the MIC of the
454 combinations decreased and, reversibly, kappa increased. Random peptide libraries are
455 combinations of multiple random AMP sequences, a feature that might be crucial and hold
456 potential for outperforming combinations of a few single AMPs.
457 The mutant selection window (MSW) is defined as the range of antimicrobial concentrations
458 where the resistant mutants are selectively favoured over susceptible strains (95). The upper
459 bound is given by the MIC of the resistant mutant, the lower bound, also known as the minimal
460 selective concentration (96), is reached when the net growth rates of the resistant and susceptible
461 strains are equal. By using random peptide libraries, such as FK20, that lead to higher kappa
462 values, in comparison to single AMP-evolved strains, could narrow the range of concentrations
463 selecting resistance (i.e. the MSW).
464
465 **Conclusions**
466 This work reinforced the idea of combinational therapy as a path for tackling antibiotic resistance,
467 highlighting the potential therapeutical capacity of random peptide libraries. Herein, a 20-mer
468 random peptide library, FK20, was shown to avoid resistance and remain sensitive after selection,
469 despite evolving mutations and fitness costs. Our findings suggest that *P. aeruginosa* detects the
470 presence of these antimicrobial agents, but for the duration of our *in vitro* selection protocol (i.e.
471 four weeks), were not able to evolve effective resistance mechanisms. Additionally, these cationic
472 and hydrophobic AMP cocktails can be synthesized affordably and have shown to be non-toxic
473 and non-haemolytic in a mouse model (21, 22).The findings herein depicted strengthen the case
474 for favouring the usage of random cocktails of AMPs over single AMPs, against which resistance
475 evolved *in vitro*.
476 In the past, promising studies have claimed novel antibiotics “resistance-proof”, able to stay
477 effective at killing their target pathogens, such as the case of Teixobactin (97), being later refuted
478 (98). Thus, despite the positive findings herein evidenced for FK20, one should side with caution.
479 Moreover, further studies should be conducted concerning the interaction of these RPMs with the
480 host innate immunity. The usage of AMPs/RPMs that strongly synergize with host innate immune
481 response should be favoured, as it could lead to an overall reduction in dosage, hence reducing

482 potential side effects (99). A synergistic strategy involving random peptide libraries and the host
483 immune response holds potential to be a cost-efficient way to reduce bacterial loads and avoid
484 resistance evolution.
485
486 **Materials & Methods**
487 Bacterial strains and growth conditions
488 All experiments were performed with the *P. aeruginosa* 14 strain (PA14; kindly provided by Yael
489 Helman) (100). This strain is defined as the ancestor strain. Prior to each experiment, strains were
490 plated on Mueller-Hinton (MH) agar plates (HiMedia), and individual colonies were picked and
491 grown in MH broth overnight at 37°C. All bacterial cells used in this study were stored in 25%
492 glycerol at -80°C.
493 Synthesis of antimicrobial peptides
494 Six different AMPs and three RPMs were selected for experimental evolution (Table S1). In
495 addition to the peptides developed in house (i.e. SLM1, SLM3, p-FdK5, p-FdK5 20/80 and FK20;
496 (22, 25, 26)), four additional AMPs were selected. Melittin is the major protein component of the
497 venom of the European honeybee (*Apis mellifera*) (101). Pexiganan is a synthetic analog of
498 magainin peptides, isolated from the skin of the African clawed frog (102). Cecropin P1 was the
499 first found mammalian cecropin, isolated from pig small intestine (103), presenting extensive
500 homology to earlier discovered insect cecropins (104). PA-13 is a short synthetic a-helical hybrid
501 peptide, inspired by cathelicidin and aurein (105). While SLM1 and SLM3 are specific palmitic
502 acid-modified 5-mer peptides, composed of L-Lysine and/or L-Phenylalanine, part of a 32-peptide
503 library, p-FdK5 and p-FdK5 20/80 are randomized 5-mers, using L-Phenylalanine and D-Lysine
504 (to the ratios of 1:1 and 1:4, respectively; Fig. S1) (25, 26). Lastly, FK20 was synthetized as
505 random peptide of L-Phenylalanine and L-Lysine (1:1 ratio) (22).
506 All peptides were synthesized by 9-fluorenylmethoxy carbonyl (Fmoc) solid-phase peptide
507 synthesis (SPPS), using a peptide synthesizer (Liberty Blue; CEM, USA). To generate lipo-RPMs
508 and SLMs, acylation was produced by bounding palmitic acid to the N-terminus of the desired
509 peptide/RPM, using the same Fmoc chemistry, albeit that overnight shaking, at room temperature,
510 was used instead of microwave irradiation (26). Upon synthesis completion, peptides were,
511 sequentially, cleaved from the resin (95% trifluoroacetic acid [TFA], 2.5% water, and 2.5%

512 triisopropylsilane [TIPS]), resuspended in double distilled water (DDW), frozen and lyophilized.
513 The resulting crude peptide was dissolved in dimethyl sulfoxide (DMSO) and purified by
514 semipreparative reversed-phase high-performance liquid chromatography (RP-HPLC), while
515 matrix-assisted laser desorption ionization–time of flight mass spectrometry (MALDI-TOF-MS)
516 was utilized for verification of the peptide mass and purity. RPMs containing phenylalanine and
517 lysine (FK20, pFdK5, pFdK5 20/80) were synthesized as previously described (21).

518 Minimum Inhibition Concentration (MIC) determination

519 MIC values were determined following a standard serial dilution protocol, as described elsewhere
520 (27). Briefly, PA14 cells were grown overnight in MH broth, at 37°C and 200 rpm. Subsequently,
521 cells were diluted 1:100 in MH broth and grown until reaching an optical density at 595 nm (OD_{595})
522 of 0.1. Then, 100 µL of 5×10^5 CFU/mL were inoculated into each well in 96-well plates that
523 contained a serial dilution of AMPs or RPMs. Each plate contained 3 replicate lines per peptide.
524 The MICs were defined as the lowest concentration at which there was inhibition of bacterial
525 growth by at least 90%, after 24h, by measuring the OD_{595}.

526 The MIC was determined on 3 occasions: 1) prior to the experiment, to determine the
527 concentration of our focal peptides to be used at the start of the experimental evolution (i.e. MIC
528 of the ancestor strain); 2) at the end of the experimental evolution, detect an increase, or
529 decrease, in the resistance of the experimentally evolved strains to our peptides of interest; 3) to
530 evaluate whether the experimental evolution of a certain treatment was accompanied by an
531 increase, or decrease, in resistance or sensitivity to another antimicrobial (i.e. cross-resistance or
532 collateral-sensitivity).

533 For time containment reasons, the design of the cross-resistance/collateral sensitivity
534 experiments are not full factorial, instead, we focussed on comparisons we found most relevant:
535 1) we exposed strains evolved in the presence of the AMPs Melittin, Pexiganan, Cecropin P1 and
536 PA13, and the RPM FK20 to each other; 2) we then exposed strains evolved in the presence of
537 palmitic acid-modified peptides to peptides of the same family, namely SLM1-, SLM3- and p-
538 FdK5-evolved strains to SLM1, SLM3, p-FdK5 and p-FdK5 20/80.

539 The MIC of evolved strains was divided by MIC of the ancestor to determine the respective fold-
540 change in comparison to the ancestor (see “Statistical Analysis” section).

541

542 Experimental evolution procedure

543 Prior to evolution with AMPs/RPMs, a PA14 colony was transferred from an MH agar plate into
544 5 mL MH broth in a 50 mL tube and incubated overnight, at 37°C and 200 rpm. Subsequently, this
545 starter culture was diluted 20-fold into a 1.5mL Eppendorf tube containing 850 µL MH broth, to
546 maintain the same headspace ratio of 96-well plates, used in the experimental evolution
547 procedure, and incubated, overnight, under the same conditions (37°C and 200 rpm). This
548 process was repeated for 7 transfers to adapt the bacteria to the experimental conditions.

549 The experimental evolution procedure was designed to exert selective pressure while avoiding
550 extinction of bacterial lines, as previously described (27). Each line was exposed to 4
551 concentrations of AMP/RPMs, according to their MIC, as follows: 1.5x, 1x, 0.5x, and 0.25x (Table
552 S1). Experiments were performed in 96-well plates, and each AMP/RPM had 3 parallel replicates
553 (sharing the same ancestral inoculum). Each plate included 8 wells with bacteria absent of
554 AMPs/RPMs, as a positive control, as well as 4 wells with just medium, as negative control. Daily,
555 10 µL of the previous plate was transferred into 190 µL of fresh medium and AMPs. Every 4 days,
556 bacteria from the highest concentration of AMP/RPM were selected and transferred into 4
557 concentrations in the new plate. MIC was doubled when growth was observed in 4 out of 6 lines
558 at the MIC or higher. The experimental evolution was carried out for 27 transfers (approx. 114
559 generations). Before every selection or MIC increment, samples were taken for fossil record in
560 25% glycerol stocks and preserved at -80°C to avoid line extinction. Spot plating was performed
561 on MH agar, containing 5 µg/mL tetracycline, to confirm growth before selection. Experimental
562 evolutions were performed twice, yielding 6 replicates per selection regime over 2 replicates of
563 the experiment.

564 Fitness cost of evolved strains

565 Bacterial cells were grown overnight in MH broth and then diluted to an OD_{595} of 0.1. For each
566 strain, 200µL of culture were transferred into 96-well plates, with 3 technical replicates. Optical
567 density (OD595) was measured every 15 min for 24 h using an Epoch 2 microplate reader
568 (BioTek). Lag time and Vmax were assessed using the plate reader software (Gen5). The values
569 measured in the experimentally evolved strains were divided by the values of their respective
570 ancestors and expressed as lag time fold-change and Vmax fold-change (see 'Statistical Analysis'
571 section).

572 DNA Isolation

573 Genomic DNA for whole genome sequencing was isolated using GeneMATRIX Bacterial and
574 Yeast genomic DNA purification kit (Roboklon, Germany) following manufacturer's instructions.
575 Four µl of 10 mg/ml freshly prepared lysozyme and lysostaphin (both from Sigma) each were
576 added into bacterial lysate. The DNA quantity and quality were estimated by measuring the optical
577 density at A260/280 using the Nanodrop spectrophotometer (Thermo Scientific) and the Qubit™
578 4 Fluorometer (Thermo Scientific).

579 Sequencing

580 At the end of each replicate of the experimental evolution experiment, 10 µL of the content of
581 each well was plated on MH agar and incubated overnight. One single colony was picked per
582 plate/well to be re-sequenced. As a reference genome, we used a *de novo* assembly of a single
583 colony of PA14 taken from our frozen stock (after overnight culture).

584 The library of the ancestor strain was sequenced on a minion (Oxford Nanopore Technologies,
585 Oxford), at 400 bps translocation speed, using a kit 14 chemistry flowcell, and the resulting raw
586 sequencing data were basecalled using Guppy model dna_r10.4.1_e8.2_400bps_sup.
587 Sequencing reads were adaptor trimmed using porechop (106) and filtered using filtlong (107) to
588 retain approximately 150-fold coverage comprising reads of at least 1000 bp. The filtered reads
589 were assembled using flye (108), which produced a single circular contig that was further polished
590 using medaka consensus (109). The remaining errors were corrected using illumina reads
591 together with polypolish (110). Finally, the start position of the assembly was adjusted to begin at
592 dnaA using circlator (111). The result was annotated with prokka (112).

593 Endpoint re-sequencing of the evolved strains was done on an Illumina HiSeq2000 with 100bp
594 paired-end reads (Wellcome Trust Centre for Human Genetics, Oxford, UK). The sequencing data
595 had a mean depth of 35.9x and a mean coverage of 76.4% at 30x depth. Sequencing Adaptors
596 were trimmed with trimmomatic (113). Snippy (114) was used to call variants using by default
597 parameters, with the annotated assembly described above as a reference sequence. The
598 Provean software tool was used to predict the effect of SNPs on the function of their target protein,
599 namely amino acid substitution or indels (40).

600

601

602 Killing Curves

603 AMP/RPM-selected strains were serially diluted (two-fold concentration gradient), starting from
604 10x MIC, in 96-well plates. Approximately, 2–3x10^6 log-phase bacteria were added to a total
605 volume of 100 ml. The plates were incubated at 37°C. As it is known that AMP-mediated killing is
606 quick (115, 116), dose-response was monitored within 60 min (6). To do so, 10 µL of bacterial
607 suspension were sampled after 5, 10, 20, 40 and 60 min., then immediately diluted in 90µL PBS
608 and plated on square solid MHA plates. These solid agar plates were transferred into a 37°C
609 incubator and incubated for 24h before counting CFUs. The same procedure was followed to
610 assess killing curves for the sensitive ancestor PA14 strain. The assays were performed in
611 triplicates.

612 Modelling killing curves – Pharmacodynamics

613 Pharmacodynamics capture the functional relationship between drug dosage and bacterial growth
614 or death. To model the killing curve, discribing the relationship between the concentration of
615 AMPs/RPMs and the killing and/or growth rate of the exposed bacteria, the Hill function was used
616 (36). This function estimates four parameters: zMIC, κ, ψ_{min}, and ψ_{max} (Fig. 4A). The zMIC is the
617 MIC estimated by fitting; κ, the Hill coefficient, depicts the steepness of the curve relating bacterial
618 growth to drug concentration; ψ_{min}, and ψ_{max} represent the minimum and maximum growth rates
619 of bacteria, respectively (see Hill function equations in supplementary methods). Growth rate and
620 killing rate of bacteria are estimated from the time-kill curves as the change of CFU over time by
621 using generalized linear regression. The data for CFU were all log transformed. The starting point
622 of linear regression was the first measurement. We then fitted the growth rate and killing rate with
623 equation 4 (see supplementary methods), based on the Markov chain Monte Carlo (MCMC)
624 method and generated the pharmacodynamic curves. Pharmacodynamic parameters of the most
625 resistant experimentally evolved strains and ancestor were estimated and a summary can be
626 found in Table S2.

627 Statistical analysis

628 All the data was analysed using the R software (117) and figures were produced using GraphPad
629 Prism, version 9 for Windows, GraphPad Software, Boston, Massachusetts USA.

630 We normalized the MICs of the different evolved strains generated in this series of experiments
631 (as well as the control strain) by dividing them with the MIC of their respective ancestors, which

632 represents the MICs before applying the selection regime. The resulting variable is a fold-change
633 in MIC ("MIC fold-change") at the end of the experimental evolution compared to the beginning.
634 Similarly, we normalized both fitness readouts duration of the lag phase (lag time) and maximum
635 slope of the bacterial growth curve (Vmax) to the readouts of the ancestor of the given evolved
636 strain by dividing the values of the evolved strains to that of their respective ancestors. The
637 resulting variable is a fold-change in Vmax and lag time during experimental evolution: Vmax fold-
638 change and lag time fold-change.
639 These response variables are therefore ratios, which are non-integer despite representing count
640 data. They showed the dispersion typical of count data, as well as a heterogeneity in the variances
641 between treatments. MIC fold-changes had a maximum of 3 digits after the comma. They were
642 multiplied by 1000 to analyse them with models fitted for a negative binomial distribution (see
643 details below), since this distribution assumes a positive and integer response variable. We
644 multiplied the lag time fold-change by 100 and rounded it up according to the value of the third
645 digit after the comma to perform a similar analysis. However, such was not the case for the Vmax
646 fold-change data which satisfied the assumptions of a Linear Mixed Model and did not require to
647 be multiplied and rounded.
648 We then analysed the MIC and lag time fold-change of single sequence AMPs and RPMs strains,
649 generated by experimental evolution, with a Generalised Linear Mixed-Effect Model (GLMM),
650 fitted for a negative binomial distribution, according to the selection regime. Since the MIC fold-
651 change was always assessed towards the antimicrobial used, as a selection pressure during
652 experimental evolution, there was no further need to include the antimicrobial towards which the
653 MIC was measured with as an explanatory variable. Since the whole experiment was replicated
654 in 2 experimental blocks, we included this experimental block as a random factor. We used the
655 ‘glmmTMB’ function of th ‘glmmTMB’ package (118). As stated above, we analysed the Vmax
656 fold-change of the resulting strains with a Linear Mixed effect Model (LMM, 'lmer' function of the
657 'lme4' package) (119), including Vmax fold-change as a response variable according to the
658 selection regime and the experimental block as a random factor.
659 Pairwise comparisons between selection regimes can be performed by eye, as previously
660 reported (120, 121): the difference between two selection regimes is deemed significant when the
661 95% confidence intervals (95CI) do not overlap more than half of their length. Effect plots for post-

662 hoc comparison between different selection regimes (estimates of the models with the
663 corresponding 95CIs) are displayed in the Supplementary Material figures S5 to S7, which were
664 generated with the 'effects' package (122, 123).
665 We next used the cross-resistance/collateral sensitivity dataset to analyse whether the presence,
666 or absence, of SNPs in the 5 genes which concentrated most of the SNPs (*lasR*, *wbp* genes,
667 *phoQ*, *tpbB* and *oprL*) affected the MIC fold-changes in the bacterial strains. We built the following
668 model for each gene/antimicrobial combination: MIC fold-change x1000 as a response variable
669 explained by presence/absence of SNP in a gene, and the experimental block as a random factor
670 ('glmmTMB' function of the 'glmmTMB' package). Since SNPs in *tpbB* and *oprL* only emerged in
671 strains from 1 of the 2 experimental blocks, we performed this analysis only in the replicate in
672 which SNPs were present, using the 'glm.nb' function of the 'MASS' package (124). We
673 considered all bacterial strains, regardless of their selection regime of origin, since the selection
674 regime, which affects the presence, or absence, of SNPs in the strains, would have been colinear
675 with the latter.
676 Correlation between kappa fold-change and MIC fold-change was assessed using Spearman's
677 test (ρ), which estimates a rank-based measure of association, through the 'cor.test' function
678 included in the 'stats' package (125).
679 Pharmacodynamics analyses were performed using Rstan (126).
680
681 **Acknowledgements**
682 The authors thank E. Bittermann for the input and assistance in setting up samples for whole-
683 genome sequencing and Ronan Murphy for critically reading the manuscript and helping with data
684 interpretation.
685
686 **Funding**
687 This work was funded by the Joint Berlin-Jerusalem Postdoctoral Fellowship Program offered by
688 the Freie Universität Berlin (FUB) and Hebrew University of Jerusalem (HUJI). The project was
689 further supported by a grant from the Volkswagen Foundation (grant no. 96517).
690
691

692 **Conflicts of interest**

693 The authors declare no competing interests.

694

695 **References**

696 1. Antimicrobial Resistance C. Global burden of bacterial antimicrobial resistance in 2019:
697 a systematic analysis. Lancet. 2022;399(10325):629-55.
698 2. Qiu D, Ke M, Zhang Q, Zhang F, Lu T, Sun L, et al. Response of microbial antibiotic
699 resistance to pesticides: An emerging health threat. Sci Total Environ. 2022;850:158057.
700 3. Lepore C, Silver L, Theuretzbacher U, Thomas J, Visi D. The small-molecule antibiotics
701 pipeline: 2014-2018. Nat Rev Drug Discov. 2019;18(10):739.
702 4. Organization WH. The evolving threat of antimicrobial resistance: options for action:
703 World Health Organization; 2012.
704 5. Czaplewski L, Bax R, Clokie M, Dawson M, Fairhead H, Fischetti VA, et al. Alternatives to
705 antibiotics-a pipeline portfolio review. Lancet Infect Dis. 2016;16(2):239-51.
706 6. Yu G, Baeder DY, Regoes RR, Rolff J. Combination Effects of Antimicrobial Peptides.
707 Antimicrob Agents Chemother. 2016;60(3):1717-24.
708 7. Zasloff M. Antimicrobial peptides of multicellular organisms. Nature.
709 2002;415(6870):389-95.
710 8. Rathinakumar R, Walkenhorst WF, Wimley WC. Broad-spectrum antimicrobial peptides
711 by rational combinatorial design and high-throughput screening: the importance of interfacial
712 activity. J Am Chem Soc. 2009;131(22):7609-17.
713 9. Axelsen PH. A chaotic pore model of polypeptide antibiotic action. Biophys J.
714 2008;94(5):1549-50.
715 10. Hancock RE. Cationic peptides: effectors in innate immunity and novel antimicrobials.
716 Lancet Infect Dis. 2001;1(3):156-64.
717 11. Rodriguez-Rojas A, Nath A, El Shazely B, Santi G, Kim JJ, Weise C, et al. Antimicrobial
718 Peptide Induced-Stress Renders Staphylococcus aureus Susceptible to Toxic Nucleoside
719 Analogs. Front Immunol. 2020;11:1686.
720 12. Yu G, Baeder DY, Regoes RR, Rolff J. Predicting drug resistance evolution: insights from
721 antimicrobial peptides and antibiotics. Proc Biol Sci. 2018;285(1874).
722 13. Perron GG, Zasloff M, Bell G. Experimental evolution of resistance to an antimicrobial
723 peptide. Proc Biol Sci. 2006;273(1583):251-6.
724 14. Spohn R, Daruka L, Lazar V, Martins A, Vidovics F, Grezal G, et al. Integrated
725 evolutionary analysis reveals antimicrobial peptides with limited resistance. Nat Commun.
726 2019;10(1):4538.
727 15. Bian X, Qu X, Zhang J, Nang SC, Bergen PJ, Tony Zhou Q, et al. Pharmacokinetics and
728 pharmacodynamics of peptide antibiotics. Adv Drug Deliv Rev. 2022;183:114171.
729 16. Liu YY, Wang Y, Walsh TR, Yi LX, Zhang R, Spencer J, et al. Emergence of plasmid-
730 mediated colistin resistance mechanism MCR-1 in animals and human beings in China: a
731 microbiological and molecular biological study. Lancet Infect Dis. 2016;16(2):161-8.
732 17. Tacconelli E, Carrara E, Savoldi A, Harbarth S, Mendelson M, Monnet DL, et al.
733 Discovery, research, and development of new antibiotics: the WHO priority list of antibiotic-
734 resistant bacteria and tuberculosis. Lancet Infect Dis. 2018;18(3):318-27.
735 18. Laxminarayan R, Duse A, Wattal C, Zaidi AK, Wertheim HF, Sumpradit N, et al. Antibiotic
736 resistance-the need for global solutions. Lancet Infect Dis. 2013;13(12):1057-98.
737 19. Tyers M, Wright GD. Drug combinations: a strategy to extend the life of antibiotics in
738 the 21st century. Nat Rev Microbiol. 2019;17(3):141-55.
739 20. Roemhild R, Bollenbach T, Andersson DI. The physiology and genetics of bacterial
740 responses to antibiotic combinations. Nat Rev Microbiol. 2022;20(8):478-90.

21. Hayouka Z, Chakraborty S, Liu R, Boersma MD, Weisblum B, Gellman SH. Interplay among subunit identity, subunit proportion, chain length, and stereochemistry in the activity profile of sequence-random peptide mixtures. J Am Chem Soc. 2013;135(32):11748-51.
22. Hayouka Z, Bella A, Stern T, Ray S, Jiang H, Grovenor CRM, et al. Binary Encoding of Random Peptide Sequences for Selective and Differential Antimicrobial Mechanisms. Angew Chem Int Ed Engl. 2017;56(28):8099-103.
23. Siriwardena TN, Gan BH, Kohler T, van Delden C, Javor S, Reymond JL. Stereorandomization as a Method to Probe Peptide Bioactivity. ACS Cent Sci. 2021;7(1):126-34.
24. Stern T, Zelinger E, Hayouka Z. Random peptide mixtures inhibit and eradicate methicillin-resistant Staphylococcus aureus biofilms. Chem Commun (Camb). 2016;52(44):7102-5.
25. Topman S, Tamir-Ariel D, Bochnic-Tamir H, Stern Bauer T, Shafir S, Burdman S, et al. Random peptide mixtures as new crop protection agents. Microb Biotechnol. 2018;11(6):1027-36.
26. Topman-Rakover S, Malach E, Burdman S, Hayouka Z. Antibacterial lipo-random peptide mixtures exhibit high selectivity and synergistic interactions. Chem Commun (Camb). 2020;56(80):12053-6.
27. Maron B, Rolff J, Friedman J, Hayouka Z. Antimicrobial Peptide Combination Can Hinder Resistance Evolution. Microbiol Spectr. 2022;10(4):e0097322.
28. Makovitzki A, Avrahami D, Shai Y. Ultrashort antibacterial and antifungal lipopeptides. Proc Natl Acad Sci U S A. 2006;103(43):15997-6002.
29. Makovitzki A, Viterbo A, Brotman Y, Chet I, Shai Y. Inhibition of fungal and bacterial plant pathogens in vitro and in planta with ultrashort cationic lipopeptides. Appl Environ Microbiol. 2007;73(20):6629-36.
30. Brotman Y, Makovitzki A, Shai Y, Chet I, Viterbo A. Synthetic ultrashort cationic lipopeptides induce systemic plant defense responses against bacterial and fungal pathogens. Appl Environ Microbiol. 2009;75(16):5373-9.
31. Pendleton JN, Gorman SP, Gilmore BF. Clinical relevance of the ESKAPE pathogens. Expert Rev Anti Infect Ther. 2013;11(3):297-308.
32. Stover CK, Pham XQ, Erwin AL, Mizoguchi SD, Warrener P, Hickey MJ, et al. Complete genome sequence of Pseudomonas aeruginosa PAO1, an opportunistic pathogen. Nature. 2000;406(6799):959-64.
33. Livermore DM. Multiple mechanisms of antimicrobial resistance in Pseudomonas aeruginosa: our worst nightmare? Clin Infect Dis. 2002;34(5):634-40.
34. Ben Hur D, Kapach G, Wani NA, Kiper E, Ashkenazi M, Smollan G, et al. Antimicrobial Peptides against Multidrug-Resistant Pseudomonas aeruginosa Biofilm from Cystic Fibrosis Patients. J Med Chem. 2022;65(13):9050-62.
35. Reynolds D, Kollef M. The Epidemiology and Pathogenesis and Treatment of Pseudomonas aeruginosa Infections: An Update. Drugs. 2021;81(18):2117-31.
36. Regoes RR, Wiuff C, Zappala RM, Garner KN, Baquero F, Levin BR. Pharmacodynamic functions: a multiparameter approach to the design of antibiotic treatment regimens. Antimicrob Agents Chemother. 2004;48(10):3670-6.
37. Witzany C, Rolff J, Regoes RR, Igler C. The pharmacokinetic-pharmacodynamic modelling framework as a tool to predict drug resistance evolution. Microbiology (Reading). 2023;169(7).
38. Pál C, Papp B, Lázár V. Collateral sensitivity of antibiotic-resistant microbes. Trends in Microbiology. 2015;23(7):401-7.
39. Imamovic L, Sommer MO. Use of collateral sensitivity networks to design drug cycling protocols that avoid resistance development. Sci Transl Med. 2013;5(204):204ra132.
40. Choi Y, Sims GE, Murphy S, Miller JR, Chan AP. Predicting the functional effect of amino acid substitutions and indels. PLoS One. 2012;7(10):e46688.

792 41. Ueda A, Wood TK. Connecting quorum sensing, c-di-GMP, pel polysaccharide, and
793 biofilm formation in Pseudomonas aeruginosa through tyrosine phosphatase TpbA (PA3885).
794 PLoS Pathog. 2009;5(6):e1000483.
795 42. Lim A, De Vos D, Brauns M, Mossialos D, Gaballa A, Qing D, et al. Molecular and
796 immunological characterization of OprL, the 18 kDa outer-membrane peptidoglycan-associated
797 lipoprotein (PAL) of Pseudomonas aeruginosa. Microbiology (Reading). 1997;143 (Pt 5):1709-
798 16.
799 43. Gambello MJ, Iglewski BH. Cloning and characterization of the Pseudomonas
800 aeruginosa lasR gene, a transcriptional activator of elastase expression. J Bacteriol.
801 1991;173(9):3000-9.
802 44. Burrows LL, Charter DF, Lam JS. Molecular characterization of the Pseudomonas
803 aeruginosa serotype O5 (PAO1) B-band lipopolysaccharide gene cluster. Mol Microbiol.
804 1996;22(3):481-95.
805 45. Larkin A, Imperiali B. Biosynthesis of UDP-GlcNAc(3NAc)A by WbpB, WbpE, and WbpD:
806 enzymes in the Wbp pathway responsible for O-antigen assembly in Pseudomonas aeruginosa
807 PAO1. Biochemistry. 2009;48(23):5446-55.
808 46. Fields PI, Groisman EA, Heffron F. A Salmonella locus that controls resistance to
809 microbicidal proteins from phagocytic cells. Science. 1989;243(4894):1059-62.
810 47. Lee JY, Ko KS. Mutations and expression of PmrAB and PhoPQ related with colistin
811 resistance in Pseudomonas aeruginosa clinical isolates. Diagn Microbiol Infect Dis.
812 2014;78(3):271-6.
813 48. Heurlier K, Denervaud V, Haenni M, Guy L, Krishnapillai V, Haas D. Quorum-sensing-
814 negative (lasR) mutants of Pseudomonas aeruginosa avoid cell lysis and death. J Bacteriol.
815 2005;187(14):4875-83.
816 49. Perfeito L, Fernandes L, Mota C, Gordo I. Adaptive mutations in bacteria: high rate and
817 small effects. Science. 2007;317(5839):813-5.
818 50. Dettman JR, Sztepanacz JL, Kassen R. The properties of spontaneous mutations in the
819 opportunistic pathogen Pseudomonas aeruginosa. BMC Genomics. 2016;17:27.
820 51. Mookherjee N, Anderson MA, Haagsman HP, Davidson DJ. Antimicrobial host defence
821 peptides: functions and clinical potential. Nat Rev Drug Discov. 2020;19(5):311-32.
822 52. Organization WH. Antibacterial agents in clinical and preclinical development: an
823 overview and analysis. World Health Organization; 2021.
824 53. Organization WH. Antibacterial agents in preclinical development: an open access
825 database. World Health Organization; 2019.
826 54. Dobson AJ, Purves J, Kamysz W, Rolff J. Comparing selection on S. aureus between
827 antimicrobial peptides and common antibiotics. PLoS One. 2013;8(10):e76521.
828 55. Habets MG, Brockhurst MA. Therapeutic antimicrobial peptides may compromise
829 natural immunity. Biol Lett. 2012;8(3):416-8.
830 56. Pena-Miller R, Laehnemann D, Jansen G, Fuentes-Hernandez A, Rosenstiel P,
831 Schulenburg H, et al. When the most potent combination of antibiotics selects for the greatest
832 bacterial load: the smile-frown transition. PLoS Biol. 2013;11(4):e1001540.
833 57. Baym M, Stone LK, Kishony R. Multidrug evolutionary strategies to reverse antibiotic
834 resistance. Science. 2016;351(6268):aad3292.
835 58. Lazar V, Martins A, Spohn R, Daruka L, Grezal G, Fekete G, et al. Antibiotic-resistant
836 bacteria show widespread collateral sensitivity to antimicrobial peptides. Nat Microbiol.
837 2018;3(6):718-31.
838 59. Barbosa C, Beardmore R, Schulenburg H, Jansen G. Antibiotic combination efficacy
839 (ACE) networks for a Pseudomonas aeruginosa model. PLoS Biol. 2018;16(4):e2004356.
840 60. Makarova O, Johnston P, Rodriguez-Rojas A, El Shazely B, Morales JM, Rolff J. Genomics
841 of experimental adaptation of Staphylococcus aureus to a natural combination of insect
842 antimicrobial peptides. Sci Rep. 2018;8(1):15359.

843 61. Ward H, Perron GG, Maclean RC. The cost of multiple drug resistance in Pseudomonas
844 aeruginosa. J Evol Biol. 2009;22(5):997-1003.
845 62. Igler C, Rolff J, Regoes R. Multi-step vs. single-step resistance evolution under different
846 drugs, pharmacokinetics, and treatment regimens. Elife. 2021;10.
847 63. Somerville GA, Chaussee MS, Morgan CI, Fitzgerald JR, Dorward DW, Reitzer LJ, et al.
848 Staphylococcus aureus aconitase inactivation unexpectedly inhibits post-exponential-phase
849 growth and enhances stationary-phase survival. Infect Immun. 2002;70(11):6373-82.
850 64. LaCroix RA, Palsson BO, Feist AM. A Model for Designing Adaptive Laboratory Evolution
851 Experiments. Appl Environ Microbiol. 2017;83(8).
852 65. Hong J, Hu J, Ke F. Experimental Induction of Bacterial Resistance to the Antimicrobial
853 Peptide Tachyplesin I and Investigation of the Resistance Mechanisms. Antimicrob Agents
854 Chemother. 2016;60(10):6067-75.
855 66. Santos-Lopez A, Fritz MJ, Lombardo JB, Burr AHP, Heinrich VA, Marshall CW, et al.
856 Evolved resistance to a novel cationic peptide antibiotic requires high mutation supply. Evol
857 Med Public Health. 2022;10(1):266-76.
858 67. Macfarlane EL, Kwasnicka A, Ochs MM, Hancock RE. PhoP-PhoQ homologues in
859 Pseudomonas aeruginosa regulate expression of the outer-membrane protein OprH and
860 polymyxin B resistance. Mol Microbiol. 1999;34(2):305-16.
861 68. McPhee JB, Lewenza S, Hancock RE. Cationic antimicrobial peptides activate a two-
862 component regulatory system, PmrA-PmrB, that regulates resistance to polymyxin B and
863 cationic antimicrobial peptides in Pseudomonas aeruginosa. Mol Microbiol. 2003;50(1):205-17.
864 69. Groisman EA. The pleiotropic two-component regulatory system PhoP-PhoQ. J
865 Bacteriol. 2001;183(6):1835-42.
866 70. Miller AK, Brannon MK, Stevens L, Johansen HK, Selgrade SE, Miller SI, et al. PhoQ
867 mutations promote lipid A modification and polymyxin resistance of Pseudomonas aeruginosa
868 found in colistin-treated cystic fibrosis patients. Antimicrob Agents Chemother.
869 2011;55(12):5761-9.
870 71. Li Y, Xia L, Chen J, Lian Y, Dandekar AA, Xu F, et al. Resistance elicited by sub-lethal
871 concentrations of ampicillin is partially mediated by quorum sensing in Pseudomonas
872 aeruginosa. Environ Int. 2021;156:106619.
873 72. Gilbert KB, Kim TH, Gupta R, Greenberg EP, Schuster M. Global position analysis of the
874 Pseudomonas aeruginosa quorum-sensing transcription factor LasR. Mol Microbiol.
875 2009;73(6):1072-85.
876 73. Sakuragi Y, Kolter R. Quorum-sensing regulation of the biofilm matrix genes (pel) of
877 Pseudomonas aeruginosa. J Bacteriol. 2007;189(14):5383-6.
878 74. Zhao K, Yang X, Zeng Q, Zhang Y, Li H, Yan C, et al. Evolution of lasR mutants in
879 polymorphic Pseudomonas aeruginosa populations facilitates chronic infection of the lung. Nat
880 Commun. 2023;14(1):5976.
881 75. Ciofu O, Mandsberg LF, Bjarnsholt T, Wassermann T, Hoiby N. Genetic adaptation of
882 Pseudomonas aeruginosa during chronic lung infection of patients with cystic fibrosis: strong
883 and weak mutators with heterogeneous genetic backgrounds emerge in mucA and/or lasR
884 mutants. Microbiology (Reading). 2010;156(Pt 4):1108-19.
885 76. Miller WL, Wenzel CQ, Daniels C, Larocque S, Brisson JR, Lam JS. Biochemical
886 characterization of WbpA, a UDP-N-acetyl-D-glucosamine 6-dehydrogenase involved in O-
887 antigen biosynthesis in Pseudomonas aeruginosa PAO1. J Biol Chem. 2004;279(36):37551-8.
888 77. Hancock RE, Mutharia LM, Chan L, Darveau RP, Speert DP, Pier GB. Pseudomonas
889 aeruginosa isolates from patients with cystic fibrosis: a class of serum-sensitive, nontypable
890 strains deficient in lipopolysaccharide O side chains. Infect Immun. 1983;42(1):170-7.
891 78. Rocchetta HL, Burrows LL, Lam JS. Genetics of O-antigen biosynthesis in Pseudomonas
892 aeruginosa. Microbiol Mol Biol Rev. 1999;63(3):523-53.

79. Joiner KA. Studies on the mechanism of bacterial resistance to complement-mediated killing and on the mechanism of action of bactericidal antibody. Curr Top Microbiol Immunol. 1985;121:99-133.
80. Dasgupta T, de Kievit TR, Masoud H, Altman E, Richards JC, Sadovskaya I, et al. Characterization of lipopolysaccharide-deficient mutants of Pseudomonas aeruginosa derived from serotypes O3, O5, and O6. Infect Immun. 1994;62(3):809-17.
81. Kadurugamuwa JL, Lam JS, Beveridge TJ. Interaction of gentamicin with the A band and B band lipopolysaccharides of Pseudomonas aeruginosa and its possible lethal effect. Antimicrob Agents Chemother. 1993;37(4):715-21.
82. Wang D, Dorosky RJ, Han CS, Lo CC, Dichosa AE, Chain PS, et al. Adaptation genomics of a small-colony variant in a Pseudomonas chlororaphis 30-84 biofilm. Appl Environ Microbiol. 2015;81(3):890-9.
83. Malone JG, Jaeger T, Spangler C, Ritz D, Spang A, Arrieumerlou C, et al. YfiBNR mediates cyclic di-GMP dependent small colony variant formation and persistence in Pseudomonas aeruginosa. PLoS Pathog. 2010;6(3):e1000804.
84. Pu M, Wood TK. Tyrosine phosphatase TpbA controls rugose colony formation in Pseudomonas aeruginosa by dephosphorylating diguanylate cyclase TpbB. Biochem Biophys Res Commun. 2010;402(2):351-5.
85. Remans K, Vercammen K, Bodilis J, Cornelis P. Genome-wide analysis and literature-based survey of lipoproteins in Pseudomonas aeruginosa. Microbiology (Reading). 2010;156(Pt 9):2597-607.
86. Panmanee W, Gomez F, Witte D, Pancholi V, Britigan BE, Hassett DJ. The peptidoglycan-associated lipoprotein OprL helps protect a Pseudomonas aeruginosa mutant devoid of the transactivator OxyR from hydrogen peroxide-mediated killing during planktonic and biofilm culture. J Bacteriol. 2008;190(10):3658-69.
87. Ghazaei C. Antibiotic Resistance Profiles of Pseudomonas aeruginosa Isolates Containing Virulence Genes. Research in Molecular Medicine. 2021;9(4):245-52.
88. Marxer M, Vollenweider V, Schmid-Hempel P. Insect antimicrobial peptides act synergistically to inhibit a trypanosome parasite. Philos Trans R Soc Lond B Biol Sci. 2016;371(1695).
89. Rolff J, Schmid-Hempel P. Perspectives on the evolutionary ecology of arthropod antimicrobial peptides. Philos Trans R Soc Lond B Biol Sci. 2016;371(1695).
90. Matsuzaki K, Mitani Y, Akada KY, Murase O, Yoneyama S, Zasloff M, et al. Mechanism of synergism between antimicrobial peptides magainin 2 and PGLa. Biochemistry. 1998;37(43):15144-53.
91. Brogden KA. Antimicrobial peptides: pore formers or metabolic inhibitors in bacteria? Nat Rev Microbiol. 2005;3(3):238-50.
92. El Shazely B, Yu G, Johnston PR, Rolff J. Resistance Evolution Against Antimicrobial Peptides in Staphylococcus aureus Alters Pharmacodynamics Beyond the MIC. Front Microbiol. 2020;11:103.
93. Zanchi C, Johnston PR, Rolff J. Evolution of defence cocktails: Antimicrobial peptide combinations reduce mortality and persistent infection. Mol Ecol. 2017;26(19):5334-43.
94. Srinivasan S, Waghu FH, Idicula-Thomas S, Venkatesh KV. A steady-state modeling approach for simulation of antimicrobial peptide-cell membrane interaction. Biochim Biophys Acta Biomembr. 2020;1862(4):183242.
95. Lazzaro BP, Zasloff M, Rolff J. Antimicrobial peptides: Application informed by evolution. Science. 2020;368(6490).
96. Gullberg E, Cao S, Berg OG, Ilback C, Sandegren L, Hughes D, et al. Selection of resistant bacteria at very low antibiotic concentrations. PLoS Pathog. 2011;7(7):e1002158.
97. Ling LL, Schneider T, Peoples AJ, Spoering AL, Engels I, Conlon BP, et al. A new antibiotic kills pathogens without detectable resistance. Nature. 2015;517(7535):455-9.

98. Lloyd DG, Schofield BJ, Goddard MR, Taylor EJ. De Novo Resistance to Arg(10)-Teixobactin Occurs Slowly and Is Costly. Antimicrob Agents Chemother. 2020;65(1).
99. Johnston PR, Makarova O, Rolff J. Inducible defenses stay up late: temporal patterns of immune gene expression in Tenebrio molitor. G3 (Bethesda). 2013;4(6):947-55.
100. He J, Baldini RL, Deziel E, Saucier M, Zhang Q, Liberati NT, et al. The broad host range pathogen Pseudomonas aeruginosa strain PA14 carries two pathogenicity islands harboring plant and animal virulence genes. Proc Natl Acad Sci U S A. 2004;101(8):2530-5.
101. Habermann E, Neumann W. Characterization of the effective components of snake venoms. Naunyn Schmiedebergs Arch Exp Pathol Pharmakol. 1954;223(5):388-98.
102. Fuchs PC, Barry AL, Brown SD. In vitro antimicrobial activity of MSI-78, a magainin analog. Antimicrob Agents Chemother. 1998;42(5):1213-6.
103. Lee JY, Boman A, Sun CX, Andersson M, Jornvall H, Mutt V, et al. Antibacterial peptides from pig intestine: isolation of a mammalian cecropin. Proc Natl Acad Sci U S A. 1989;86(23):9159-62.
104. Hultmark D, Steiner H, Rasmuson T, Boman HG. Insect immunity. Purification and properties of three inducible bactericidal proteins from hemolymph of immunized pupae of Hyalophora cecropia. Eur J Biochem. 1980;106(1):7-16.
105. Klubthawee N, Adisakwattana P, Hanpithakpong W, Somsri S, Aunpad R. A novel, rationally designed, hybrid antimicrobial peptide, inspired by cathelicidin and aurein, exhibits membrane-active mechanisms against Pseudomonas aeruginosa. Sci Rep. 2020;10(1):9117.
106. Wick R. Porechop: adapter trimmer for Oxford Nanopore reads. 2018.
107. Wick RR, Menzel P. Filtlong. 2018.
108. Kolmogorov M, Yuan J, Lin Y, Pevzner PA. Assembly of long, error-prone reads using repeat graphs. Nat Biotechnol. 2019;37(5):540-6.
109. Nanoporetech. Medaka: Sequence correction provided by ONT research. GitHub 2019 [Available from: https://github.com/nanoporetech/medaka.
110. Wick RR, Holt KE. Polypolish: Short-read polishing of long-read bacterial genome assemblies. PLoS Comput Biol. 2022;18(1):e1009802.
111. Hunt M, Silva ND, Otto TD, Parkhill J, Keane JA, Harris SR. Circlator: automated circularization of genome assemblies using long sequencing reads. Genome Biol. 2015;16:294.
112. Seemann T. Prokka: rapid prokaryotic genome annotation. Bioinformatics. 2014;30(14):2068-9.
113. Bolger AM, Lohse M, Usadel B. Trimmomatic: a flexible trimmer for Illumina sequence data. Bioinformatics. 2014;30(15):2114-20.
114. Seemann T. Snippy: fast bacterial variant calling from NGS reads. 2015.
115. Sochacki KA, Barns KJ, Bucki R, Weisshaar JC. Real-time attack on single Escherichia coli cells by the human antimicrobial peptide LL-37. Proc Natl Acad Sci U S A. 2011;108(16):E77-81.
116. Rangarajan N, Bakshi S, Weisshaar JC. Localized permeabilization of E. coli membranes by the antimicrobial peptide Cecropin A. Biochemistry. 2013;52(38):6584-94.
117. Team RC. R: A language and environment for statistical computing. Vienna, Austria; 2020.
118. Brooks ME, Kristensen K, Van Benthem KJ, Magnusson A, Berg CW, Nielsen A, et al. glmmTMB balances speed and flexibility among packages for zero-inflated generalized linear mixed modeling. The R journal. 2017;9(2):378-400.
119. Bates D, Mächler M, Bolker B, Walker S. Fitting Linear Mixed-Effects Models Using lme4. Journal of Statistical Software. 2015;67(1):1 - 48.
120. Cumming G, Finch S. Inference by eye: confidence intervals and how to read pictures of data. Am Psychol. 2005;60(2):170-80.
121. Cumming G. Inference by eye: reading the overlap of independent confidence intervals. Stat Med. 2009;28(2):205-20.
122. Fox J. Effect Displays in R for Generalised Linear Models. Journal of Statistical Software. 2003;8(15):1 - 27.

123. Fox J, Weisberg S. An R companion to applied regression: Sage publications; 2018.
124. Venables WN, Ripley BD. Modern applied statistics with S. 4th ed: Springer, New York; 2002.
125. Best DJ, Roberts DE. Algorithm AS 89: The Upper Tail Probabilities of Spearman's Rho. Journal of the Royal Statistical Society Series C (Applied Statistics). 1975;24(3):377-9.
126. Team SD. RStan: The R interface to Stan. R package version 2.17. 3. Online: http://mc-stanorg. 2018.